Cell PRESS
Chemistry & Biology
Article

Sequence Determinants of a Specific Inactive Protein Kinase Conformation

Sanjay B. Hari,[1] Ethan A. Merritt,[2] and Dustin J. Maly[1,*]
[1]Department of Chemistry
[2]Department of Biochemistry
University of Washington, Seattle, WA 98195, USA
*Correspondence: maly@chem.washington.edu
http://dx.doi.org/10.1016/j.chembiol.2013.05.005

SUMMARY

Only a small percentage of protein kinases have been shown to adopt a distinct inactive ATP-binding site conformation, called the Asp-Phe-Gly-out (DFG-out) conformation. Given the high degree of homology within this enzyme family, we sought to understand the basis of this disparity on a sequence level. We identified two residue positions that sensitize mitogen-activated protein kinases (MAPKs) to inhibitors that stabilize the DFG-out inactive conformation. After characterizing the structure and dynamics of an inhibitor-sensitive MAPK mutant, we demonstrated the generality of this strategy by sensitizing a kinase (apoptosis signal-regulating kinase 1) not in the MAPK family to several DFG-out stabilizing ligands, using the same residue positions. The use of specific inactive conformations may aid the study of noncatalytic roles of protein kinases, such as binding partner interactions and scaffolding effects.

INTRODUCTION

Protein kinases represent approximately 2% of all human genes (Manning et al., 2002a), a testament to the vast number of kinase-mediated signal transduction pathways. Immunity, cell cycle regulation, and morphogenesis are only a few of the processes controlled by protein kinases (Manning et al., 2002b). Aberrant kinase activity can lead to diseases, such as cancer and inflammation (Noble et al., 2004); thus, normal cell function is reliant on precise kinase regulation, the basis of which lies in the interconversion between active and inactive catalytic states.

The catalytic domains of protein kinases are composed of a larger, mainly α helical C-terminal lobe and a smaller N-terminal lobe composed mainly of β strands. The active site is located in a cleft between these two lobes. A flexible polypeptide called the activation loop resides on the outer edge of the active site and often contains serine, threonine, or tyrosine residues that can be phosphorylated (Canagarajah et al., 1997). Activation loop phosphorylation often results in a dramatic increase in a kinase's catalytic activity (Zhang et al., 2008; Zhou and Zhang, 2002).

Catalytically active kinase conformations are highly conserved, owing to the evolutionary pressure of functional preservation. Inactive conformations, however, lack this pressure and are more varied across the kinase family. While the exact number of discrete inactive conformations is not known (although believed to be limited [Jura et al., 2011]), only a few have been observed crystallographically in multiple kinases. Small-molecule kinase inhibitors have played a large role in determining active-site conformational accessibility by stabilizing specific active site conformations. For example, structural characterization of the drug imatinib bound to its target kinase Abl (Schindler et al., 2000; Zimmermann et al., 1997) revealed that this inhibitor stabilizes a specific inactive conformation that is characterized by the unique orientation of the highly conserved Asp-Phe-Gly (DFG) motif at the base of Abl's activation loop. In Abl's active conformation (DFG-in), the aspartate side chain of the DFG motif faces into the active site to facilitate catalysis. Additionally, its neighboring phenylalanine residue occupies a hydrophobic pocket adjacent to the ATP-binding site. In contrast, the activation loop of the observed inactive form (DFG-out) undergoes a significant translocation that moves the catalytic aspartate out of the active site and the phenylalanine away from the hydrophobic pocket. Since the initial observation that imatinib stabilizes the DFG-out conformation of Abl, a number of ATP-competitive ligands that stabilize this conformation in other protein kinases have been identified (Davis et al., 2011; Liu and Gray, 2006).

Although the overall topologies of kinase active sites are well conserved across this enzyme family, less than 10% have been observed in the DFG-out conformation (Zuccotto et al., 2010), and most examples are tyrosine kinases (DiMauro et al., 2006; Hodous et al., 2007; Mol et al., 2004; Schindler et al., 2000; Wan et al., 2004), despite serine/threonine (S/T) kinases constituting a majority of the human kinome (Manning et al., 2002a). Furthermore, the few S/T kinases that have been shown to adopt this conformation appear to be outliers in their own subfamilies. For example, the mitogen-activated protein kinase (MAPK) p38α was one of the first kinases to be characterized in the DFG-out conformation, and numerous structures of this kinase bound to conformation-specific ligands that stabilize this inactive form have been reported (Angell et al., 2008; Pargellis et al., 2002). However, p38δ, which is in the same MAPK subfamily and more than 61% identical in sequence (Remy et al., 2010), is insensitive to ligands that selectively recognize this conformation (Sullivan et al., 2005). Furthermore, there is no experimental evidence that other closely related MAPKs, such

as extracellular signal-regulated kinase 1/2 (Erk1/2) and c-Jun N-terminal kinase 3 (Jnk3), possess the ability to adopt the DFG-out conformation (Fox et al., 1998; Xie et al., 1998; Zhang et al., 1994).

Based on the information above, two main questions arise. First, can p38α adopt the DFG-out inactive conformation because of only a few sequence differences from the other MAPKs, or is this ability due to more global determinants in kinase tertiary structure? Second, how do sequence differences contribute to ligand binding? That is, can all kinases adopt the DFG-out inactive conformation given the appropriate ligand and simply the energetics of known ligands that stabilize the DFG-out conformation cause them to prefer p38α, or can p38α access a unique conformational space that is somehow productive toward ligand binding? Unfortunately, structural studies provide no information about the dynamics or plasticity of kinases. To wit, a reported crystal structure of the *apo* form of inactive p38α adopts the DFG-in conformation (Wang et al., 1997), giving no indication of its ability to adopt the DFG-out conformation. Further confounding is that *apo* forms do exist of other kinases in the DFG-out conformation (Griffith et al., 2004; Hubbard et al., 1994).

Here, we report the identification of two specific residues that allow MAPKs to adopt the DFG-out inactive conformation. We show that mutagenesis at these positions yields kinases that are sensitive to general ligands that stabilize this inactive conformation. Additionally, we provide structural evidence that an inhibitor-sensitive mutant of Erk2 can adopt the DFG-out inactive conformation. Next, using isotope-coded affinity tagging (ICAT) experiments, we show that these mutations change the dynamics of the segment of the activation loop next to the DFG motif. Finally, we extend our observations to the distantly related yeast sterile (STE) group kinase apoptosis signal-regulating kinase 1 (ASK1) to demonstrate that these two residues are relevant to S/T kinases outside the MAPK family. This sensitization strategy may be used to study the effects of inactive conformations in various noncatalytic roles of protein kinases, including scaffolding complexes (Therrien et al., 1996) and binding partner interactions (Rodríguez and Crespo, 2011).

RESULTS AND DISCUSSION

A Small-Molecule Probe Reveals Binding Preference among MAPKs

ATP-competitive inhibitors have proven to be invaluable reagents for studying the conformational accessibility of protein kinase active sites. Most of these ligands, known as "type I" inhibitors, are able to bind to the active form of kinase ATP-binding sites, where all conserved catalytic residues are in the proper orientation for catalysis. However, a growing number of ligands have been identified that selectively stabilize ATP-binding site conformations that are not compatible with catalysis. These ligands occupy regions within the kinase that are only accessible through the displacement of conserved catalytic residues. For example, inhibitors that stabilize the helix αC-out inactive conformation induce a rotation of helix αC that disrupts the catalytically important salt bridge between a glutamate residue on helix αC and a lysine residue on the N-lobe beta sheet (Krishnamurty et al., 2013; Wood et al., 2004).

Another more commonly observed inactive conformation is the DFG-out inactive conformation described earlier. Ligands that stabilize this conformation (type II) have substituents that extend into a hydrophobic pocket (Figure 1A) normally occupied by the conserved phenylalanine of the DFG motif when kinases are in an active conformation. The translocation of the phenylalanine residue perturbs the position of the neighboring catalytic aspartate of the DFG motif. Type II ligands also contain a linkage that connects the substituents that occupy the adenosine and DFG-out pockets, which makes two additional hydrogen bonds with a backbone residue in the DFG motif (Asp) and a conserved glutamate residue located in helix αC. Only in the DFG-out inactive conformation, whereby the DFG motif phenylalanine is removed from the DFG-out pocket, can a kinase active site make the interactions described above with a type II inhibitor.

The reasons for the far fewer examples of S/T kinases in the DFG-out inactive conformation, relative to tyrosine kinases, are not known. We felt that the high sequence homology of the MAPKs and the general availability of diverse ligands that stabilize the DFG-out conformation of p38α made this kinase group ideal for probing the sequence and structural determinants of ATP-binding site conformational accessibility. First, we confirmed biophysically that MAPKs other than p38α are not sensitive to type II inhibitors, and thus are most likely unable to adopt the DFG-out inactive conformation, with a fluorescently labeled affinity reagent F that we have previously described (Figure 1B; Ranjitkar et al., 2010). This reagent consists of a general ligand for the DFG-out conformation linked to a BODIPY fluorophore. Upon binding to kinases that are able to adopt the DFG-out conformation, this probe demonstrates a significant increase in fluorescence. Direct measurement of binding affinity rather than enzymatic inhibition allows kinase conformational accessibility to be determined independent of enzyme activity or phosphorylation state. Because specific phosphorylation events have been shown to affect the conformational equilibrium of some kinases, this assay simplifies biochemical analysis (Seeliger et al., 2007). The binding affinities of the unphosphorylated forms of the MAPKs p38α, p38δ, Jnk3, and Erk2 were determined for BODIPY-conjugated probe F (Figure 1C; Table 1). Consistent with previous structural studies and inhibitor screens, only p38α bound tightly (K_d = 15 nM) to the probe.

One distinguishing characteristic of type II inhibitors is that they display slow association and dissociation kinetics when interacting with the ATP-binding sites of protein kinases (Gruenbaum et al., 2009; Pargellis et al., 2002). This rate is slower than that of type I inhibitors, owing to the significant conformational change that must occur in order to accommodate type II ligands. By monitoring the loss of fluorescent signal of kinase-bound F in the presence of a nonfluorescent competitor, the dissociative half-life ($t_{1/2}$) of p38α was determined. Probe F dissociates slowly from the active site of p38α (Figure 1D; Table 1), comparable to studies with other type II ligands (Gruenbaum et al., 2009; Pargellis et al., 2002; Sullivan et al., 2005).

Two Active Site Residues Affect MAPK Sensitivity to Type II Inhibitors

Given that closely related kinases greatly differ in their sensitivities to a general type II ligand, we sought to determine the sequence basis for this disparity. We confined our search to a

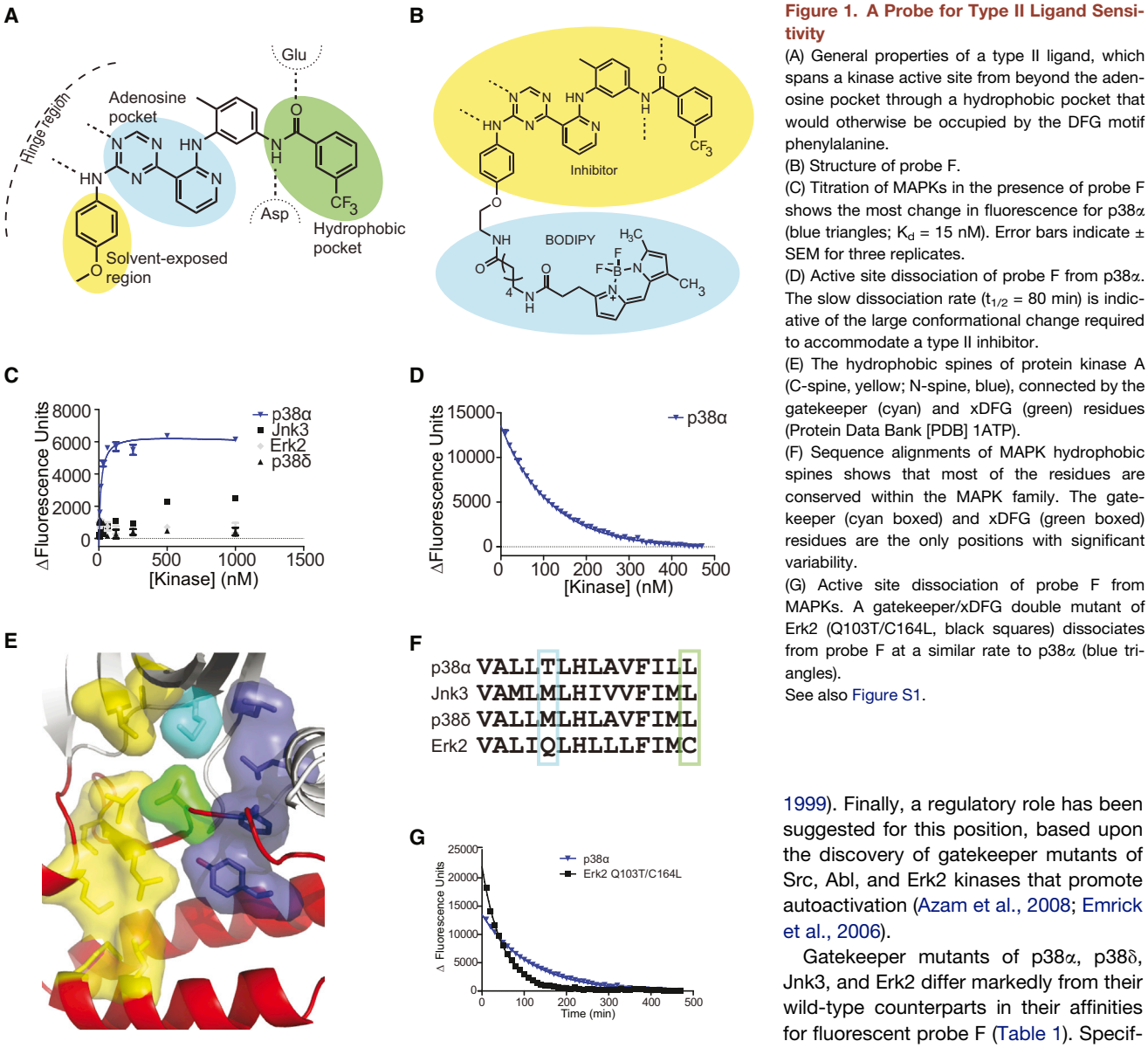

Figure 1. A Probe for Type II Ligand Sensitivity

(A) General properties of a type II ligand, which spans a kinase active site from beyond the adenosine pocket through a hydrophobic pocket that would otherwise be occupied by the DFG motif phenylalanine.

(B) Structure of probe F.

(C) Titration of MAPKs in the presence of probe F shows the most change in fluorescence for p38α (blue triangles; K_d = 15 nM). Error bars indicate ± SEM for three replicates.

(D) Active site dissociation of probe F from p38α. The slow dissociation rate ($t_{1/2}$ = 80 min) is indicative of the large conformational change required to accommodate a type II inhibitor.

(E) The hydrophobic spines of protein kinase A (C-spine, yellow; N-spine, blue), connected by the gatekeeper (cyan) and xDFG (green) residues (Protein Data Bank [PDB] 1ATP).

(F) Sequence alignments of MAPK hydrophobic spines shows that most of the residues are conserved within the MAPK family. The gatekeeper (cyan boxed) and xDFG (green boxed) residues are the only positions with significant variability.

(G) Active site dissociation of probe F from MAPKs. A gatekeeper/xDFG double mutant of Erk2 (Q103T/C164L, black squares) dissociates from probe F at a similar rate to p38α (blue triangles).

See also Figure S1.

series of hydrophobic residues that form two spatially conserved hydrophobic spines in kinases that are in the active conformation (Kornev et al., 2006, 2008; Kornev and Taylor, 2010; Figure 1E). While almost all of the residues in the hydrophobic spines of p38α, p38δ, Jnk3, and Erk2 are identical, one residue that connects these spines is more varied (Figure 1F). This position, known as the "gatekeeper" residue, blocks access to a hydrophobic pocket adjacent to the site of ATP binding. The gatekeeper residue has been the subject of considerable study. A number of drug-resistant kinase mutants with altered gatekeeper residues have been identified in the clinic, including breakpoint cluster region (BCR)-Abl T315I (Quintás-Cardama and Cortes, 2008), epidermal growth factor receptor T790M (Kobayashi et al., 2005), and KIT T670I (Tamborini et al., 2004). Furthermore, conversion of the gatekeeper from a larger to a smaller alanine or glycine residue has been used to confer sensitivity to a series of orthogonal kinase inhibitors (Bishop et al., 1999). Finally, a regulatory role has been suggested for this position, based upon the discovery of gatekeeper mutants of Src, Abl, and Erk2 kinases that promote autoactivation (Azam et al., 2008; Emrick et al., 2006).

Gatekeeper mutants of p38α, p38δ, Jnk3, and Erk2 differ markedly from their wild-type counterparts in their affinities for fluorescent probe F (Table 1). Specifically, the p38δ M107T and Jnk3 M146I gatekeeper mutants exhibited low nanomolar affinities for the probe. Conversely, the T106Q gatekeeper mutant of p38α abrogated binding to this probe (K_d > 1000 nM). Curiously, the Erk2 Q103T and Q103A gatekeeper mutants showed increased binding to the fluorescent probe but not to the extent demonstrated by the p38δ or Jnk3 gatekeeper mutants. Therefore, we looked for other positions that differ between Erk2 and the other MAPKs tested. Our attention was drawn to the residue immediately preceding the DFG motif (xDFG), which, like the gatekeeper residue, connects the two hydrophobic spines. The identity of this residue is cysteine in Erk2 but leucine in p38α, p38δ, and Jnk3. Mutating the xDFG position to leucine (C164L) in Erk2 Q103T and Q103A produced Erk2 variants (Q103T/C164L and Q103A/C164L) with increased affinities for probe F (K_d = 40 nM and 13 nM, respectively). Further, probe F demonstrated slow dissociative half-lives for all of these sensitized variants (Figure 1G; Table 1). Thus, it appears that the identities of the two residues

Table 1. Binding Affinity Data of Probe F to MAPKs

Kinase	Probe K_d (nM)	Dissociative $t_{1/2}$ (min)
p38α wild-type (WT)	15 ± 2	79.6 ± 0.2
p38α T106Q	>1,000	n/d
Jnk3 WT	n/c[a]	n/d
Jnk3 M146I	10 ± 2	51.8 ± 0.2
Erk2 WT	>1,000	n/d
Erk2 Q103T	n/c[a]	n/d
Erk2 Q103A	n/c[a]	n/d
Erk2 Q103T/C164L	40 ± 10	33 ± 1
Erk2 Q103A/C164L	13 ± 7	27.8 ± 1.0
p38δ WT	>1,000	n/d
p38δ M107T	38 ± 5	26.3 ± 0.4

n/d, not determined.
[a]Data were not convergent to a plateau and thus could not be accurately fit to a curve.

that connect the hydrophobic spines of MAPKs determine their sensitivities to type II inhibitors and may influence their abilities to adopt the DFG-out conformation.

Having determined MAPK residues that modulate probe F binding, we were curious to know whether these positions affected only the pharmacophore of this fluorescent ligand or corresponded more broadly to other ligands that stabilize the DFG-out inactive conformation. Therefore, we tested their enzymatic inhibition by a series of diverse type II ligands. In order to do so, it was necessary to activate the MAPKs with their respective MAPK kinases (MEKs). All MAPK variants were significantly activated by their upstream MEKs, and Michaelis constants (K_m[ATP]) of the activated MAPKs were not dramatically different between wild-type and mutant kinases (Table 2).

A structurally diverse panel of type II inhibitors that are potent inhibitors of p38α with varied structures but all of the features of a general ligand for the DFG-out conformation (Figure 2) were tested in activity assays: Iclusig (L1) is an inhibitor of wild-type and drug-resistant forms of the oncogenic tyrosine kinase BCR-Abl (Huang et al., 2010). L2 is derived from a series of aminoquinazoline inhibitors that target the Src-family kinase Lck (DiMauro et al., 2006; Brigham et al., 2013). The ATP-competitive pharmacophore (L3) component of fluorescent probe F was also tested (Seeliger et al., 2009). Finally, we included a pyrazolourea (L4) inhibitor of p38α that only occupies the hydrophobic binding pocket created by the movement of the DFG motif to an inactive conformation (Dumas et al., 2000). Even with the structural diversity of this ligand set, it is possible that some kinases that are able to adopt the DFG-out conformation will not be sensitive to these inhibitors. Consistent with the binding studies using probe F, only p38α was potently inhibited by all of the type II inhibitors tested (Table 2). Hence, ligands that stabilize the DFG-out inactive conformation appear to be ineffective toward the other MAPKs, despite extensive structural and sequence homology. However, the probe-sensitized kinase mutants of p38δ, Jnk3, and Erk2 were inhibited by low nanomolar concentrations of virtually all of the inhibitors in our panel. Thus, the gatekeeper and xDFG positions appear to control the sensitivity of MAPKs to pharmacophores that stabilize the DFG-out inactive conformation.

It is important to note that alanine, glycine, and isoleucine gatekeeper mutants of Jnk3 all have high affinities for probe F (Figure S1A available online). An isoleucine side chain is larger than threonine and, in fact, occupies almost the same volume as methionine (Esque et al., 2010); therefore, the presence of a small residue at the gatekeeper position is not mandatory for type II inhibitor sensitivity. Nonetheless, both isoleucine and threonine are branched at their β carbon positions, so we speculated that they may be similar enough to be equally tolerated at the gatekeeper position in other MAPKs. Indeed, p38α T106I binds equipotently to probe F as the wild-type (Figure S1B), and while p38δ M107I is not as sensitive to inhibitors L1–L4 as M107T, it is notably more so than the wild-type (Figure S1C). Positional comparisons among the few S/T kinases that have been characterized to adopt the DFG-out conformation reveal several gatekeeper residues, including a phenylalanine in CDK6 (Figure S1D). This diversity further illustrates that threonine is not the only gatekeeper residue that permits type II inhibitor sensitivity. However, it appears that methionine and glutamine at this position strongly disfavor type II ligand inhibition, which is noteworthy, as these two residues combined represent almost

Table 2. Inhibition Data for Kinases against Type II Inhibitors

		K_i (nM)			
Kinase	K_m(ATP) (μM)	L1	L2	L3	L4
p38α WT	229 ± 16	8.1 ± 0.2	<2[a]	8.0 ± 0.4	6.4 ± 1.6
p38α T106Q	>1,000[b]	3,700 ± 400	1,120 ± 20	>10,000	55 ± 4
Erk2 WT	120 ± 10	>10,000	>10,000	>10,000	>10,000
Erk2 Q103T	83 ± 5	>10,000	10.8 ± 0.8	310 ± 20	>10,000
Erk2 Q103T/C164L	180 ± 20	4,200 ± 600	4.7 ± 0.3	28.4 ± 1.7	6,600 ± 700
Erk2 Q103A/C164L	137 ± 6	1,490 ± 50	<2[a]	36 ± 4	1,100 ± 300
Jnk3 WT	8.3 ± 0.6	1,300 ± 300	106 ± 9	101.6 ± 1.6	660 ± 90
Jnk3 M146I	66 ± 3	67 ± 3	1.65 ± 0.05	5.9 ± 0.5	155 ± 9
p38δ WT	91 ± 6	5,800 ± 400	>10,000	>10,000	>10,000
p38δ M107T	380 ± 40	54 ± 5	3.62 ± 0.18	26 ± 2	37.5 ± 0.6

[a]Assay was performed with 2 nM kinase.
[b]Rate of reaction maintained linearity as high as 1,000 μM ATP.

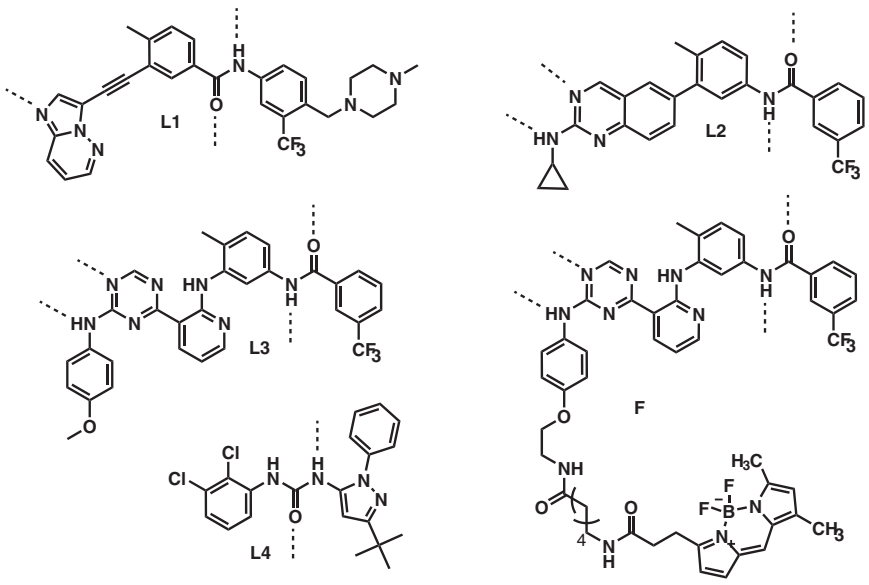

Figure 2. Structures of L1–L4 and Probe F
Despite varied structures, all of these inhibitors stabilize the DFG-out inactive conformation. Polar contacts are shown with dashed lines.

half of all gatekeeper residues in human kinases (Zhang et al., 2005).

Structural Evidence for DFG-Out Conformational Accessibility

L1–L4 are conformation-selective inhibitors, in that the ATP-binding sites of protein kinases most likely need to adopt the DFG-out conformation in order to accommodate these ligands. To ensure that this is the case, we determined the crystal structure of Erk2 Q103A/C164L bound to the type II ligand L2 (Table S1). Consistent with the increased sensitivity of this kinase mutant to type II inhibitors, the refined structure shows that the phenylalanine residue in the DFG motif (Phe-166) undergoes a large translocation; displacing the catalytic Asp from an orientation that is competent for catalysis (Figure 3A). Also, as expected, L2 is buried within the ATP-binding cleft of this Erk2 mutant and makes all of the characteristic contacts of a type II inhibitor (Figure 3B). The 2-aminoquinazoline scaffold makes similar hydrophobic contacts as the adenine ring of ATP and forms two hydrogen bonds with the hinge region. The 3-trifluoromethylphenyl moiety of L2 occupies the hydrophobic pocket created by movement of the DFG motif phenylalanine side chain, and the amide linker forms hydrogen bonds with the backbone of Asp-165 in the DFG motif and the side chain of Glu-69 in helix αC.

Most of the activation loop is well resolved, including the TEY activation motif. Superimposition of this structure with that of inactive Erk2 in the DFG-in conformation (Zhang et al., 1994) shows a dramatic difference in activation loop configuration (Figure 3C), including a translocation of 9.9 Å by the DFG phenylalanine residue. Also of note is the position of the TEY motif: not only are these residues on opposite sides of the active site from those in the DFG-in conformation but Tyr-185 appears to be involved in a pi-stacking interaction with Phe-166. Interestingly, p38α bound to pyrazolourea L4 in the DFG-out conformation shows no such interaction (Figure 3D), although the similar position of its activation loop with that of Erk2 Q103A/C164L corroborates the hypothesis made by Sullivan et al. that kinases in the DFG-out conformation cannot be activated by their upstream kinases because the position of their TxY motif renders their activation loops to be inaccessible to MEKs (Sullivan et al., 2005).

Gatekeeper Mutations Alter the Dynamics of the Activation Loop

Having demonstrated that inhibitor-sensitive Erk2 can adopt the DFG-out inactive conformation, we explored how this change affects its dynamic properties. One possibility is that type II inhibitor-sensitized kinases can sample the same conformational space as their wild-type counterparts, and the introduction of gatekeeper and xDFG mutations eliminate unfavorable interactions that prevent inhibitor binding. Alternatively, the introduced mutations could allow p38δ, Jnk3, and Erk2 to access new conformational states that are compatible with favorable type II ligand binding. Normally, nuclear magnetic resonance (NMR) experiments can be used to test hypotheses about protein dynamics. However, previous reports have shown that kinase activation loops move on an "intermediate" time scale, rendering them unresolvable by NMR, due to line broadening (Langer et al., 2004; Vogtherr et al., 2006). Therefore, we used ICAT footprinting reagents to probe the active site dynamics of Erk2 Q103T/C164L. This mass spectrometry-based technique measures the alkylation rates of cysteine residues to determine their solvent exposures. ICAT footprinting is complementary to hydrogen-deuterium exchange (HX) footprinting because, while it lacks the ability to measure dynamic changes of the entire protein in a single experiment, it has the advantage of resolution, since it follows specific residues rather than peptic fragments. We mutated five individual residues in the active site of Erk2 Q103T/C164L and compared their alkylation rates to those of the single mutant C164L (Figure 4A). This mutant was used as a control instead of wild-type Erk2 to allow a direct comparison of the contribution of the gatekeeper residue. Erk2 C164L has no measureable affinity to probe F, making it an appropriate wild-type substitute (data not shown).

Two of the five positions examined showed altered alkylation rates between Erk2 C164L and Q103T/C164L (Figure 4B). Position 82 is located close to the gatekeeper residue, meaning that the observed rate change is likely due to local steric effects of the mutated gatekeeper residue. However, position 172 is on the activation loop of Erk2 and quite distant from the gatekeeper. A rate change at this position suggests the activation loop of the type II ligand-sensitized mutant (Q103T/C164L) can access different states than the wild-type surrogate (C164L). It also appears that this motion is localized to the region around the DFG motif, since no rate change was observed for positions further along the activation loop. To validate this result, we performed

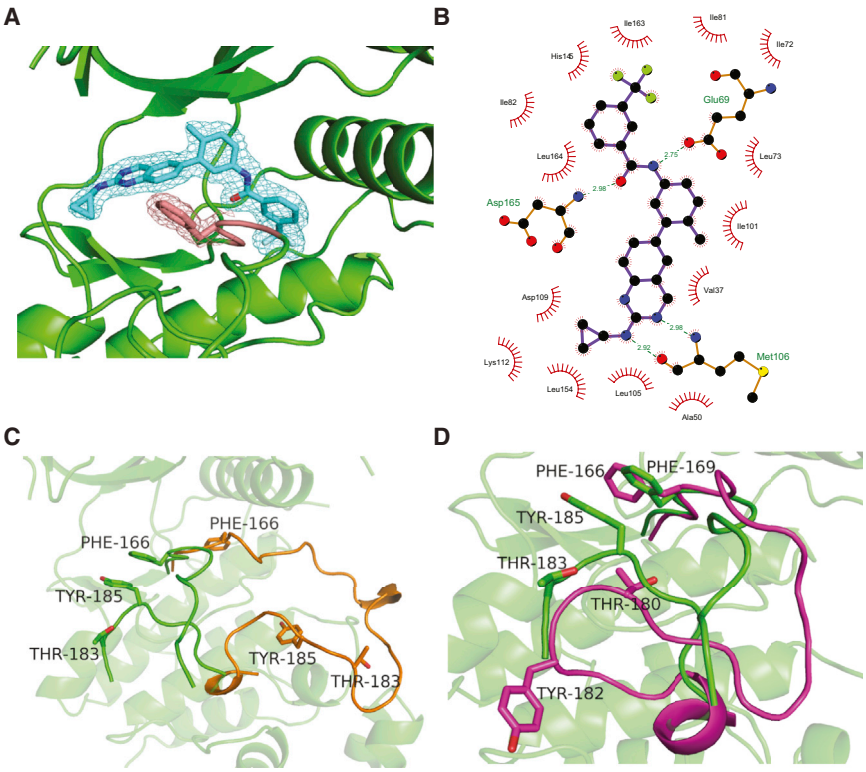

Figure 3. L2-Bound Erk2 Q103A/C164L Adopts the DFG-Out Inactive Conformation
(A) Erk2 Q103A/C164L with L2 (cyan) and Phe-166 (salmon) contoured at 1.0 σ. Part of the N-lobe beta sheet is hidden for clarity.
(B) Interaction map of L2 in the active site of Erk2 Q103A/C164L. Map generated by LigPlot+ (Laskowski and Swindells, 2011).
(C) Superimposition of L2-bound Erk2 Q103A/C164L (green) with *apo* inactive Erk2 (orange; activation loop shown only) (PDB 1ERK) reveals a large activation loop translocation.
(D) Superimposition of L2-bound Erk2 Q103A/C164L (green) with L4-bound p38α (magenta; activation loop shown only) (PDB 2BAJ). No pi-stacking is observed between Phe-169 and Tyr-182 in p38α.
See also Table S1.

the same experiment on Erk2 Q103A/C164L and found an equivalent effect. These results suggest that the identity of a kinase's gatekeeper residue affects the conformational preference of its activation loop in the *apo* form.

The rate change in position 172 between wild-type surrogate and inhibitor-sensitive Erk2 is apparent but subtle. Molecular dynamics simulations on both short and long time scales have modeled DFG-out-adopting kinases moving fully into the DFG-out conformation within nanoseconds (Frembgen-Kesner and Elcock, 2006; Shan et al., 2009); thus, it might be expected that such a large translocation would produce a more significant alkylation rate difference. However, structural analysis shows that, despite the large translocation of the activation loop between the DFG-out and DFG-in conformations, the degree of solvent exposure of most of the residues (including position 172) remains the same. Therefore, a vastly different rate difference cannot be expected between residues occupying similar environments.

It is also important to note that, while our data suggest that inhibitor-sensitive Erk2 has an altered activation loop conformational preference relative to wild-type Erk2, this does not necessarily mean that the DFG-out conformation of the *apo* form of this enzyme is substantially populated in the absence of ligand. Such would imply that ligands that stabilize the DFG-out conformation bind via a conformational selection mechanism (Boehr et al., 2006; Tsai et al., 1999) rather than an induced-fit mechanism (Koshland, 1958). While kinetics and molecular dynamics calculations provide strong supporting evidence that type II inhibitors bind to the ATP-binding sites of kinases by a conformational selection mechanism (Shan et al., 2009), we can only conclude from our data that our MAPK mutants have an altered conformational preference that is more conducive to ligand binding than the wild-type.

In a previous study by Emrick et al., several mutations that were predicted to allow increased movement of a hydrophobic core of residues in the active site of Erk2, including the Q103A gatekeeper mutant, result in increased autophosphorylation (Emrick et al., 2006). HX footprinting of one of these Erk2 mutants, I84A, showed that a portion of the activation loop had substantially increased mobility. These observations are consistent with the increased sensitivity of Erk2 Q103A/C164L to type II inhibitors. However, the dynamic difference we observed in position 172 between wild-type surrogate and inhibitor-sensitive Erk2 did not appear in Erk2 I84A from the HX footprinting experiment. Furthermore, liquid chromatography/mass spectrometry (MS) data revealed that, unlike the Q103A and Q103T single mutants, recombinant Erk2 Q103T/C164L and Q103A/C164L expressed in *E. coli* were not phosphorylated at either residue of the TEY activation motif (Figure S2). These observations suggest that the dynamic differences observed in our footprinting experiments are independent of any autophosphorylation capability and thus need not be consistent with the HX study by Emrick et al. Furthermore, the I84A mutant, previously shown to undergo a high rate of autophosphorylation (Emrick et al., 2006), showed negligible binding to our fluorescent probe (data not shown), refuting the possibility that autophosphorylation capability and DFG-out conformational accessibility are correlated. Interestingly, the I84A/C164L mutant showed very little autophosphorylation, suggesting that position 164 is a general switch that downregulates autophosphorylation.

To our knowledge, the only study to examine the xDFG position was by Martin et al., who targeted this residue in the development of new type II inhibitors for Aurora A kinase (Martin et al., 2012). However, the DFG motif itself has been studied intensely. The catalytic aspartate of this motif makes critical polar contacts with type II inhibitors; thus, it is reasonable that a large adjacent residue may hinder its ability to make these contacts. However, in the case of the Erk2 Q103T/C164L double mutant, leucine is considered to be larger in size (Esque et al., 2010) and similar

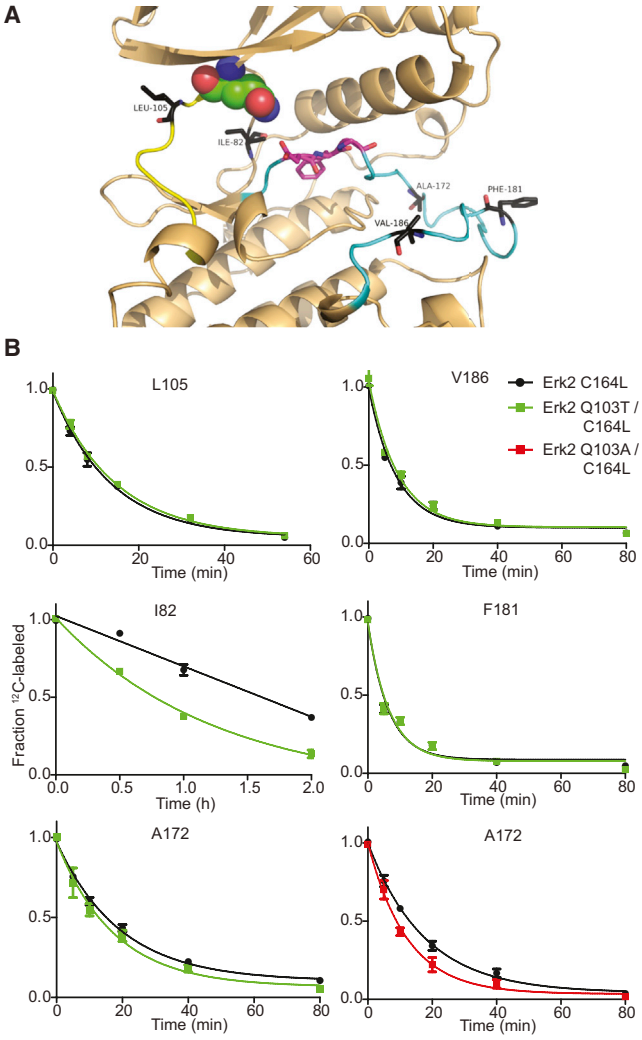

Figure 4. ICAT Footprinting of Inhibitor-Sensitive and Inhibitor-Insensitive Erk2

(A) Residue positions studied (black sticks). The hinge region (yellow), activation loop (cyan), DFG motif (magenta sticks), and gatekeeper residue (spheres) are also shown (PDB 1ERK).

(B) Footprinting time courses. The proximity of position 82 to the gatekeeper provides the explanation that a smaller gatekeeper residue, as in the case of Erk2 Q103T/C164L, would provide greater solvent accessibility and a faster alkylation rate. Position 172, however, is far from the gatekeeper and still shows altered rates for both Erk Q103T/C164L and Q103A/C164L. Error bars indicate ± SEM for three replicates.

See also Figures S2 and S3.

in hydrophobicity (Kyte and Doolittle, 1982) compared to cysteine. Furthermore, we found that mutating the xDFG position from leucine to cysteine in the inhibitor-sensitive Jnk3 M146I mutant abolishes binding to probe F (Figure S3A). Therefore, in conjunction with the gatekeeper residue, this position appears to play a role in the DFG-out conformational accessibility of protein kinases.

The Gatekeeper and xDFG Mutations Are General

In a recent proteomic screen using a type II inhibitor to identify kinases that can adopt the DFG-out conformation, we identified the S/T kinase Stk10 (LOK) (Ranjitkar et al., 2010). Stk10 resides in the STE kinase group, whose human members are homologous to yeast Ste20 kinase (Record et al., 2010) but share little sequence similarity to MAPKs (Figure 5A). Enrichment of Stk10 with resin-coupled L3 and nanomolar affinity of purified recombinant kinase to BODIPY-conjugated probe F corroborated this result. Furthermore, we found that Stk10 was sensitive to the panel of type II inhibitors described above (Figure 5C). Finally, a crystal structure was recently solved of Stk10 in the DFG-out inactive conformation (Ranjitkar et al., 2012; Figure 5B), making it one of only a handful of S/T kinases outside the MAPK family to be structurally characterized in this form.

To test whether our observations for MAPKs are general, we turned to another kinase in the STE group, ASK1. Unlike Stk10, this closely related kinase showed no measureable binding to our BODIPY-labeled inhibitor or enzymatic inhibition by any of the type II inhibitors in our panel (Figure 5C). Therefore, ASK1 provided an ideal candidate to test the generality of using the gatekeeper and xDFG positions to alter DFG-out conformational accessibility. Mutating the gatekeeper position of ASK1 from a methionine to a threonine residue generated an ASK1 mutant (M754T) that has a dissociation constant of 1.3 μM for probe F (Figure S3B). Encouraged by this result, we also mutated the xDFG position and found that the M754T/S821C double mutant bound to this probe with a K_d of 50 nM (Figure 5C). Enzymatic activity assays using this mutant showed that almost all of the small molecules in our type II panel exhibited nanomolar inhibition of this kinase. These data strongly suggest the generality of the gatekeeper and xDFG positions as mediators of the DFG-out inactive conformation.

SIGNIFICANCE

More than 10 years after its discovery, the DFG-out inactive conformation appears to be accessible by only a handful of protein kinases. Given the significant interest in exploiting the hydrophobic pocket exposed in this conformation to gain a selectivity advantage, it is a worthwhile endeavor to determine if the DFG-out conformation is accessible to all kinases given the proper inhibitor or if the accessibility of this conformation is limited by the dynamic properties of the kinase itself. However, such studies are difficult to control, due to the often significant sequence disparity between protein kinases.

We have demonstrated that two residue positions in the active site of protein kinases appear to modulate their sensitivity to inhibitors that stabilize the DFG-out inactive conformation. Specifically, we showed that mutations at these positions conferred the ability to adopt the DFG-out conformational state that was disfavored in the wild-type kinase. This effect was demonstrated for the MAPK family as well as the distantly related STE kinase family, suggesting a general trend across many protein kinases.

Our footprinting experiments suggest that the dynamics of kinases that can adopt the DFG-out conformation are different from those that cannot. However, more research is required to fully discern the dynamic nature of these kinases. Concurrently, our strategy may be used to rapidly sensitize kinases to type II ligands and study

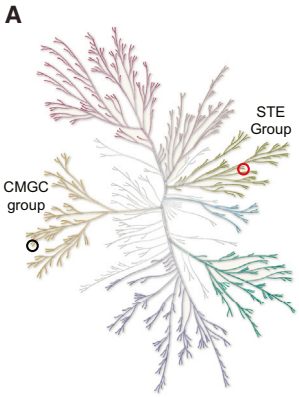

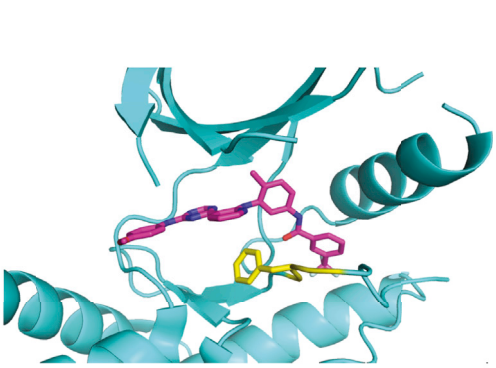

C

	IC$_{50}$ (nM)					
	Ponatinib	GP17	DSA7	Pyrazolourea	Probe K$_d$ (nM)	Diss. t$_{1/2}$ (min)
Stk10	10.0 ± 0.5	22 ± 1	8 ± 1	210 ± 20	30 ± 8	68 ± 1
ASK1 wt	>10,000	>10,000	>10,000	n/d	>2,000	n/d
ASK1 M754T/S821C	27 ± 2	7.7 ± 0.4	116 ± 5	**n/d**	50 ± 10	30 ± 1

Figure 5. The Gatekeeper/xDFG Sensitization Strategy Is General

(A) Kinome dendrogram with the S/T kinases p38α (black) and Stk10 (red) circled illustrates the distant relationship between the two kinases. Kinome illustration reproduced courtesy of Cell Signaling Technology (http://www.cellsignal.com).

(B) Stk10 bound to L3 (magenta) in the DFG-out conformation with activation loop (yellow; F176 in sticks) highlighted (PDB 4EQU).

(C) Inhibition data of STE group kinases against inhibitors L1–L4 and binding and dissociation data of probe F. The ASK1 gatekeeper/xDFG double mutant (M754T/S821C) is inhibited at nanomolar levels for all inhibitors tested and binds to probe F with nanomolar affinity. n/d, not determined.

conformationally dependent effects of scaffolding and other noncatalytic functions.

EXPERIMENTAL PROCEDURES

Cloning

Genes for mouse p38α, human ASK1, and human Stk10 (S. Knapp) were provided in bacterial expression vectors. Genes for human Jnk3, mouse p38δ (R. Davis), and rat Erk2 (J. Blenis) were cloned into His$_6$ vector pMCSG7 (M. Donnelly). Genes for human MEK6, human MEK4, human MEK7 (R. Davis), human MEK2 (P. Khavari), and human Map3k1 (G. Johnson) were cloned into His$_6$-glutathione S-transferase (GST) vector pMCSG10 (M. Donnelly). Mutagenesis was performed by Quikchange (Agilent). Plasmids were isolated from cultures grown from single colonies and sequenced. Primers used for cloning and mutagenesis are available upon request.

Protein Expression and Purification

Detailed procedures are in the Supplemental Information.

Small Molecule Synthesis

Detailed procedures and commercial suppliers are in the Supplemental Information.

Fluorescent Probe Measurements

These experiments were performed as described (Hari et al., 2012; Ranjitkar et al., 2010).

Kinase Activation and Activity Assays

ASK1 and Stk10 were catalytically active after purification. MAPKs were activated as follows prior to use in activity assays: kinase was incubated in phosphorylation buffer (50 mM 3-(N-morpholino)propanesulfonic acid [pH 7.4], 10 mM $MgCl_2$, 1 mM dithiothreitol [DTT], 0.001% [v/v] Tween 20) with BSA (0.1 mg/ml), ATP (1.3 mM), and upstream kinase (MEK6 for p38α and -δ, MEK2 for Erk2, and Map3k1+MEK4+MEK7 for Jnk3) for 1 hr at room temperature.

Activated kinase was incubated with inhibitor (4% in DMSO, 10 μM starting concentration, then 3-fold dilutions to 0.5 nM) in kinase reaction buffer (50 mM 4-(2-hydroxyethyl)-1-piperazineethanesulfonic acid [pH 7.5], 60 mM $MgCl_2$, 1 mM EGTA) with BSA (50 μg/ml), myelin basic protein (0.2 mg/ml), sodium orthovanadate (2 mM), cold ATP (13 μM), and γ^{32}P ATP (PerkinElmer) (0.2 μCi/well) and spotted onto a phosphocellulose membrane (Whatman). Enzyme concentrations and incubation times varied by kinase based on enzyme linearity. The membrane was washed four times with 0.05% phosphoric acid, dried, and exposed overnight to a phosphor screen (GE Healthcare). The screen was then scanned by a phosphor scanner, and spots were quantitated using ImageQuant software. K_i values were determined by nonlinear regression using Graphpad Prism software.

Kinetics

Erk2 wild-type, Q103T/C164L, and Q103A/C164L were coexpressed with constitutively active GST-MEK2 and purified as above to yield activated, ATP-free kinase. Other kinases were expressed, purified, and activated as above but then desalted using Zeba spin columns (Pierce) to remove ATP. Activity assays were performed as described above but with different concentrations of ATP (typically 1.6 μM cold ATP with 3.2 μCi γ^{32}P ATP starting concentrations, then 2-fold dilutions to 12.5 μM cold ATP with 25 nCi γ^{32}P ATP). K_m values were determined by nonlinear regression using Graphpad Prism software.

Mass Spectrometry

Kinases (75 pmol) were precipitated with 0.02% sodium deoxycholate and 10% trichloroacetic acid on ice for 10 min. The mixture was centrifuged at 4°C for 15 min, and the pellet was washed with cold acetone. After centrifugation, the pellet was resuspended in 30 μl of 200 mM Tris (pH 8.0), 8 M urea, and 2.4 mM iodoacetamide, and incubated in the dark for 30 min. The solution was then diluted with 210 μl 200 mM Tris (pH 8.0), 5.7 mM $CaCl_2$, and 1 μg/μl porcine trypsin (L-(tosylamido-2-phenyl) ethyl chloromethyl ketone treated, Sigma) and incubated at 37°C overnight. Sample (0.3 pmol) was injected onto a Thermo Scientific Dionex Acclaim Pepmap100 NanoLC capillary column (C_{18}, 150 mm length, infective dose 75 μm, 3 μm particle size) connected inline to a Finnigan liquid chromatography quadrupole mass spectrometer. Peptides of interest were identified by MS/MS data (Sequest), and corresponding extracted ion chromatograph peaks were integrated.

ICAT Footprinting

Positions chosen for study were mutated to cysteine using site-directed mutagenesis. Kinases were purified as described above but desalted into 50 mM Tris pH 8.0, 50 mM KCl, 5 mM $MgCl_2$, and 0.5 mM Tris(2-carboxyethyl)phosphine hydrochloride. Heavy labeling reagent was added to protein solutions (3 μM), and aliquots were taken at specified times and quenched with excess DTT. Samples were then prepared and analyzed by mass spectrometry as described above, except light labeling reagent was used instead of iodoacetamide. Alkylation curves were fit using GraphPad Prism software.

Crystallography

Detailed procedures are in the Supplemental Information.

ACCESSION NUMBERS

The Protein Data Bank accession number for the inhibitor-bound Erk2 Q103A/C164L structure reported in this paper is 4I5H.

SUPPLEMENTAL INFORMATION

Supplemental Information includes Supplemental Experimental Procedures, three figures, and one table and can be found with this article online at http://dx.doi.org/10.1016/j.chembiol.2013.05.005.

ACKNOWLEDGMENTS

We thank B. Gayani K. Perera, and Pratistha Ranjitkar for providing several inhibitors and Martin Sadilek and Stewart Turley for technical assistance with mass spectrometry and crystallography, respectively. This work was supported by the NIH (R01 GM086858 to D.J.M.), Alfred P. Sloan and Camille and Henry Dreyfus Foundations (to D.J.M.), and a predoctoral fellowship from the American Heart Association (to S.B.H.).

Received: March 7, 2013
Revised: April 18, 2013
Accepted: May 9, 2013
Published: June 20, 2013

REFERENCES

Angell, R.M., Angell, T.D., Bamborough, P., Bamford, M.J., Chung, C.W., Cockerill, S.G., Flack, S.S., Jones, K.L., Laine, D.I., Longstaff, T., et al. (2008). Biphenyl amide p38 kinase inhibitors 4: DFG-in and DFG-out binding modes. Bioorg. Med. Chem. Lett. *18*, 4433–4437.

Azam, M., Seeliger, M.A., Gray, N.S., Kuriyan, J., and Daley, G.Q. (2008). Activation of tyrosine kinases by mutation of the gatekeeper threonine. Nat. Struct. Mol. Biol. *15*, 1109–1118.

Bishop, A.C., Kung, C., Shah, K., Witucki, L., Shokat, K.M., and Liu, Y. (1999). Generation of monospecific nanomolar tyrosine kinase inhibitors via a chemical genetic approach. J. Am. Chem. Soc. *121*, 627–631.

Boehr, D.D., McElheny, D., Dyson, H.J., and Wright, P.E. (2006). The dynamic energy landscape of dihydrofolate reductase catalysis. Science *313*, 1638–1642.

Brigham, J.L., Perera, B.G.K., and Maly, D.J. (2013). A hexylchloride-based catch-and-release system for chemical proteomic applications. ACS Chem. Biol. *8*, 691–699.

Canagarajah, B.J., Khokhlatchev, A., Cobb, M.H., and Goldsmith, E.J. (1997). Activation mechanism of the MAP kinase ERK2 by dual phosphorylation. Cell *90*, 859–869.

Davis, M.I., Hunt, J.P., Herrgard, S., Ciceri, P., Wodicka, L.M., Pallares, G., Hocker, M., Treiber, D.K., and Zarrinkar, P.P. (2011). Comprehensive analysis of kinase inhibitor selectivity. Nat. Biotechnol. *29*, 1046–1051.

DiMauro, E.F., Newcomb, J., Nunes, J.J., Bemis, J.E., Boucher, C., Buchanan, J.L., Buckner, W.H., Cee, V.J., Chai, L., Deak, H.L., et al. (2006). Discovery of aminoquinazolines as potent, orally bioavailable inhibitors of Lck: synthesis, SAR, and in vivo anti-inflammatory activity. J. Med. Chem. *49*, 5671–5686.

Dumas, J., Hatoum-Mokdad, H., Sibley, R., Riedl, B., Scott, W.J., Monahan, M.K., Lowinger, T.B., Brennan, C., Natero, R., Turner, T., et al. (2000). 1-Phenyl-5-pyrazolyl ureas: potent and selective p38 kinase inhibitors. Bioorg. Med. Chem. Lett. *10*, 2051–2054.

Emrick, M.A., Lee, T., Starkey, P.J., Mumby, M.C., Resing, K.A., and Ahn, N.G. (2006). The gatekeeper residue controls autoactivation of ERK2 via a pathway of intramolecular connectivity. Proc. Natl. Acad. Sci. USA *103*, 18101–18106.

Esque, J., Oguey, C., and de Brevern, A.G. (2010). A novel evaluation of residue and protein volumes by means of Laguerre tessellation. J. Chem. Inf. Model. *50*, 947–960.

Fox, T., Coll, J.T., Xie, X., Ford, P.J., Germann, U.A., Porter, M.D., Pazhanisamy, S., Fleming, M.A., Galullo, V., Su, M.S., and Wilson, K.P. (1998). A single amino acid substitution makes ERK2 susceptible to pyridinyl imidazole inhibitors of p38 MAP kinase. Protein Sci. *7*, 2249–2255.

Frembgen-Kesner, T., and Elcock, A.H. (2006). Computational sampling of a cryptic drug binding site in a protein receptor: explicit solvent molecular dynamics and inhibitor docking to p38 MAP kinase. J. Mol. Biol. *359*, 202–214.

Griffith, J., Black, J., Faerman, C., Swenson, L., Wynn, M., Lu, F., Lippke, J., and Saxena, K. (2004). The structural basis for autoinhibition of FLT3 by the juxtamembrane domain. Mol. Cell *13*, 169–178.

Gruenbaum, L.M., Schwartz, R., Woska, J.R., Jr., DeLeon, R.P., Peet, G.W., Warren, T.C., Capolino, A., Mara, L., Morelock, M.M., Shrutkowski, A., et al. (2009). Inhibition of pro-inflammatory cytokine production by the dual p38/JNK2 inhibitor BIRB796 correlates with the inhibition of p38 signaling. Biochem. Pharmacol. *77*, 422–432.

Hari, S.B., Ranjitkar, P., and Maly, D.J. (2012). Determination of the kinetics and thermodynamics of ligand binding to a specific inactive conformation in protein kinases. Methods Mol. Biol. *928*, 153–159.

Hodous, B.L., Geuns-Meyer, S.D., Hughes, P.E., Albrecht, B.K., Bellon, S., Caenepeel, S., Cee, V.J., Chaffee, S.C., Emery, M., Fretland, J., et al. (2007). Synthesis, structural analysis, and SAR studies of triazine derivatives as potent, selective Tie-2 inhibitors. Bioorg. Med. Chem. Lett. *17*, 2886–2889.

Huang, W.S., Metcalf, C.A., Sundaramoorthi, R., Wang, Y., Zou, D., Thomas, R.M., Zhu, X., Cai, L., Wen, D., Liu, S., et al. (2010). Discovery of 3-[2-(imidazo[1,2-b]pyridazin-3-yl)ethynyl]-4-methyl-N-4-[(4-methylpiperazin-1-yl) methyl]-3-(trifluoromethyl)phenylbenzamide (AP24534), a potent, orally active pan-inhibitor of breakpoint cluster region-abelson (BCR-ABL) kinase including the T315I gatekeeper mutant. J. Med. Chem. *53*, 4701–4719.

Hubbard, S.R., Wei, L., Ellis, L., and Hendrickson, W.A. (1994). Crystal structure of the tyrosine kinase domain of the human insulin receptor. Nature *372*, 746–754.

Jura, N., Zhang, X., Endres, N.F., Seeliger, M.A., Schindler, T., and Kuriyan, J. (2011). Catalytic control in the EGF receptor and its connection to general kinase regulatory mechanisms. Mol. Cell *42*, 9–22.

Kobayashi, S., Boggon, T.J., Dayaram, T., Jänne, P.A., Kocher, O., Meyerson, M., Johnson, B.E., Eck, M.J., Tenen, D.G., and Halmos, B. (2005). EGFR mutation and resistance of non-small-cell lung cancer to gefitinib. N. Engl. J. Med. *352*, 786–792.

Kornev, A.P., and Taylor, S.S. (2010). Defining the conserved internal architecture of a protein kinase. Biochim. Biophys. Acta *1804*, 440–444.

Kornev, A.P., Haste, N.M., Taylor, S.S., and Eyck, L.F. (2006). Surface comparison of active and inactive protein kinases identifies a conserved activation mechanism. Proc. Natl. Acad. Sci. USA *103*, 17783–17788.

Kornev, A.P., Taylor, S.S., and Ten Eyck, L.F. (2008). A helix scaffold for the assembly of active protein kinases. Proc. Natl. Acad. Sci. USA *105*, 14377–14382.

Koshland, D.E. (1958). Application of a Theory of Enzyme Specificity to Protein Synthesis. Proc. Natl. Acad. Sci. USA *44*, 98–104.

Krishnamurty, R., Brigham, J.L., Leonard, S.E., Ranjitkar, P., Larson, E.T., Dale, E.J., Merritt, E.A., and Maly, D.J. (2013). Active site profiling reveals coupling between domains in SRC-family kinases. Nat. Chem. Biol. *9*, 43–50.

Kyte, J., and Doolittle, R.F. (1982). A simple method for displaying the hydropathic character of a protein. J. Mol. Biol. *157*, 105–132.

Langer, T., Vogtherr, M., Elshorst, B., Betz, M., Schieborr, U., Saxena, K., and Schwalbe, H. (2004). NMR backbone assignment of a protein kinase catalytic domain by a combination of several approaches: application to the catalytic subunit of cAMP-dependent protein kinase. ChemBioChem *5*, 1508–1516.

Laskowski, R.A., and Swindells, M.B. (2011). LigPlot+: multiple ligand-protein interaction diagrams for drug discovery. J. Chem. Inf. Model. *51*, 2778–2786.

Liu, Y., and Gray, N.S. (2006). Rational design of inhibitors that bind to inactive kinase conformations. Nat. Chem. Biol. *2*, 358–364.

Manning, G., Whyte, D.B., Martinez, R., Hunter, T., and Sudarsanam, S. (2002a). The protein kinase complement of the human genome. Science *298*, 1912–1934.

Manning, G., Plowman, G.D., Hunter, T., and Sudarsanam, S. (2002b). Evolution of protein kinase signaling from yeast to man. Trends Biochem. Sci. *27*, 514–520.

Martin, M.P., Zhu, J.Y., Lawrence, H.R., Pireddu, R., Luo, Y., Alam, R., Ozcan, S., Sebti, S.M., Lawrence, N.J., and Schönbrunn, E. (2012). A novel mechanism by which small molecule inhibitors induce the DFG flip in Aurora A. ACS Chem. Biol. *7*, 698–706.

Mol, C.D., Dougan, D.R., Schneider, T.R., Skene, R.J., Kraus, M.L., Scheibe, D.N., Snell, G.P., Zou, H., Sang, B.C., and Wilson, K.P. (2004). Structural basis for the autoinhibition and STI-571 inhibition of c-Kit tyrosine kinase. J. Biol. Chem. *279*, 31655–31663.

Noble, M.E., Endicott, J.A., and Johnson, L.N. (2004). Protein kinase inhibitors: insights into drug design from structure. Science *303*, 1800–1805.

Pargellis, C., Tong, L., Churchill, L., Cirillo, P.F., Gilmore, T., Graham, A.G., Grob, P.M., Hickey, E.R., Moss, N., Pav, S., and Regan, J. (2002). Inhibition of p38 MAP kinase by utilizing a novel allosteric binding site. Nat. Struct. Biol. *9*, 268–272.

Quintás-Cardama, A., and Cortes, J. (2008). Therapeutic options against BCR-ABL1 T315I-positive chronic myelogenous leukemia. Clin. Cancer Res. *14*, 4392–4399.

Ranjitkar, P., Brock, A.M., and Maly, D.J. (2010). Affinity reagents that target a specific inactive form of protein kinases. Chem. Biol. *17*, 195–206.

Ranjitkar, P., Perera, B.G., Swaney, D.L., Hari, S.B., Larson, E.T., Krishnamurty, R., Merritt, E.A., Villén, J., and Maly, D.J. (2012). Affinity-based probes based on type II kinase inhibitors. J. Am. Chem. Soc. *134*, 19017–19025.

Record, C.J., Chaikuad, A., Rellos, P., Das, S., Pike, A.C., Fedorov, O., Marsden, B.D., Knapp, S., and Lee, W.H. (2010). Structural comparison of human mammalian ste20-like kinases. PLoS ONE *5*, e11905.

Remy, G., Risco, A.M., Iñesta-Vaquera, F.A., González-Terán, B., Sabio, G., Davis, R.J., and Cuenda, A. (2010). Differential activation of p38MAPK isoforms by MKK6 and MKK3. Cell. Signal. *22*, 660–667.

Rodríguez, J., and Crespo, P. (2011). Working without kinase activity: phosphotransfer-independent functions of extracellular signal-regulated kinases. Sci. Signal. *4*, re3.

Schindler, T., Bornmann, W., Pellicena, P., Miller, W.T., Clarkson, B., and Kuriyan, J. (2000). Structural mechanism for STI-571 inhibition of abelson tyrosine kinase. Science *289*, 1938–1942.

Seeliger, M.A., Nagar, B., Frank, F., Cao, X., Henderson, M.N., and Kuriyan, J. (2007). c-Src binds to the cancer drug imatinib with an inactive Abl/c-Kit conformation and a distributed thermodynamic penalty. Structure *15*, 299–311.

Seeliger, M.A., Ranjitkar, P., Kasap, C., Shan, Y., Shaw, D.E., Shah, N.P., Kuriyan, J., and Maly, D.J. (2009). Equally potent inhibition of c-Src and Abl by compounds that recognize inactive kinase conformations. Cancer Res. *69*, 2384–2392.

Shan, Y., Seeliger, M.A., Eastwood, M.P., Frank, F., Xu, H., Jensen, M.O., Dror, R.O., Kuriyan, J., and Shaw, D.E. (2009). A conserved protonation-dependent switch controls drug binding in the Abl kinase. Proc. Natl. Acad. Sci. USA *106*, 139–144.

Sullivan, J.E., Holdgate, G.A., Campbell, D., Timms, D., Gerhardt, S., Breed, J., Breeze, A.L., Bermingham, A., Pauptit, R.A., Norman, R.A., et al. (2005). Prevention of MKK6-dependent activation by binding to p38α MAP kinase. Biochemistry *44*, 16475–16490.

Tamborini, E., Bonadiman, L., Greco, A., Albertini, V., Negri, T., Gronchi, A., Bertulli, R., Colecchia, M., Casali, P.G., Pierotti, M.A., and Pilotti, S. (2004). A new mutation in the KIT ATP pocket causes acquired resistance to imatinib in a gastrointestinal stromal tumor patient. Gastroenterology *127*, 294–299.

Therrien, M., Michaud, N.R., Rubin, G.M., and Morrison, D.K. (1996). KSR modulates signal propagation within the MAPK cascade. Genes Dev. *10*, 2684–2695.

Tsai, C.J., Kumar, S., Ma, B., and Nussinov, R. (1999). Folding funnels, binding funnels, and protein function. Protein Sci. *8*, 1181–1190.

Vogtherr, M., Saxena, K., Hoelder, S., Grimme, S., Betz, M., Schieborr, U., Pescatore, B., Robin, M., Delarbre, L., Langer, T., et al. (2006). NMR characterization of kinase p38 dynamics in free and ligand-bound forms. Angew. Chem. Int. Ed. Engl. *45*, 993–997.

Wan, P.T., Garnett, M.J., Roe, S.M., Lee, S., Niculescu-Duvaz, D., Good, V.M., Jones, C.M., Marshall, C.J., Springer, C.J., Barford, D., and Marais, R.; Cancer Genome Project. (2004). Mechanism of activation of the RAF-ERK signaling pathway by oncogenic mutations of B-RAF. Cell *116*, 855–867.

Wang, Z., Harkins, P.C., Ulevitch, R.J., Han, J., Cobb, M.H., and Goldsmith, E.J. (1997). The structure of mitogen-activated protein kinase p38 at 2.1-A resolution. Proc. Natl. Acad. Sci. USA *94*, 2327–2332.

Wood, E.R., Truesdale, A.T., McDonald, O.B., Yuan, D., Hassell, A., Dickerson, S.H., Ellis, B., Pennisi, C., Horne, E., Lackey, K., et al. (2004). A unique structure for epidermal growth factor receptor bound to GW572016 (Lapatinib): relationships among protein conformation, inhibitor off-rate, and receptor activity in tumor cells. Cancer Res. *64*, 6652–6659.

Xie, X., Gu, Y., Fox, T., Coll, J.T., Fleming, M.A., Markland, W., Caron, P.R., Wilson, K.P., and Su, M.S. (1998). Crystal structure of JNK3: a kinase implicated in neuronal apoptosis. Structure *6*, 983–991.

Zhang, F., Strand, A., Robbins, D., Cobb, M.H., and Goldsmith, E.J. (1994). Atomic structure of the MAP kinase ERK2 at 2.3 A resolution. Nature *367*, 704–711.

Zhang, C., Kenski, D.M., Paulson, J.L., Bonshtien, A., Sessa, G., Cross, J.V., Templeton, D.J., and Shokat, K.M. (2005). A second-site suppressor strategy for chemical genetic analysis of diverse protein kinases. Nat. Methods *2*, 435–441.

Zhang, Y.Y., Mei, Z.Q., Wu, J.W., and Wang, Z.X. (2008). Enzymatic activity and substrate specificity of mitogen-activated protein kinase p38alpha in different phosphorylation states. J. Biol. Chem. *283*, 26591–26601.

Zhou, B., and Zhang, Z.Y. (2002). The activity of the extracellular signal-regulated kinase 2 is regulated by differential phosphorylation in the activation loop. J. Biol. Chem. *277*, 13889–13899.

Zimmermann, J., Buchdunger, E., Mett, H., Meyer, T., and Lydon, N.B. (1997). Potent and selective inhibitors of the Abl-kinase: phenylamino-pyrimidine (PAP) derivatives. Bioorg. Med. Chem. Lett. *7*, 187–192.

Zuccotto, F., Ardini, E., Casale, E., and Angiolini, M. (2010). Through the "gatekeeper door": exploiting the active kinase conformation. J. Med. Chem. *53*, 2681–2694.